

Models of stress fluctuations in granular media

P. Claudin, J.-P. Bouchaud
Service de Physique de l'Etat Condensé,
CEA, Orme des Merisiers,
91191 Gif-sur-Yvette, Cedex France.

M. E. Cates and J. P. Wittmer
Department of Physics and Astronomy,
University of Edinburgh, JCMB King's Buildings,
Mayfield Road, Edinburgh EH9 3JZ, UK.

March 2, 2018

Abstract

We investigate in detail two models describing how stresses propagate and fluctuate in granular media. The first one is a scalar model where only the vertical component of the stress tensor is considered. In the continuum limit, this model is equivalent to a *diffusion equation* (where the rôle of time is played by the vertical coordinate) plus a randomly varying convection term. We calculate the response and correlation function of this model, and discuss several properties, in particular related to the stress distribution function. We then turn to the tensorial model, where the basic starting point is a *wave equation* which, in the absence of disorder, leads to a ray-like propagation of stress. In the presence of disorder, the rays acquire a diffusive width and the angle of propagation is shifted. A striking feature is that the response function becomes negative, which suggests that the contact network is mechanically unstable to very weak perturbations. The stress correlation function reveals characteristic features related to the ray-like propagation, which are absent in the scalar description. Our analytical calculations are confirmed and extended by a numerical analysis of the stochastic wave equation.

1 Introduction

Granular media are materials where stress fluctuations are large, even on scales much larger than the grain size. Repeatedly pouring the very same amount of powder in a silo results in fluctuations of the weight supported by the bottom plate of 20% or more [1, 2]. This weight furthermore changes very abruptly when temperature changes by only a few $^{\circ}C$, which induces only very small changes of the size of each grain [2, 3].

More quantitative experiments were recently performed by Liu et al. [4], Brockbank et al. [5] and Mueth et al. [6], where the local fluctuations of the normal stress deep inside a silo or at the base of a sandpile were measured (see also [7], and for early qualitative experiments [8]). It was found that the stress probability distribution is rather broad (i.e. the relative fluctuations are of order one), decaying exponentially for large stresses. A simple ‘scalar’ model for stress propagation was introduced and studied in detail [4, 9], which predicts a stress probability distribution in good agreement with experimental (and numerical) data. However, this model only considers the *vertical* normal component of the stress tensor, and discards all the other components: in this sense the model is scalar.

A fully ‘tensorial’ model for stress propagation in homogeneous granular media was proposed in [10, 11, 12] to account for the pressure ‘dip’ which is observed experimentally below the apex of conical sandpiles. The most striking feature of this model is that the stress propagation equation is a *wave equation*, with the vertical axis playing the rôle of time. Correspondingly, the stress propagates (in two dimensions, see [10]) along two rays which makes a certain angle with the vertical axis (the ‘light cone’). This must be contrasted with the scalar model, where stresses travel essentially vertically, which predicts a central pressure ‘hump’ (rather than a ‘dip’).

It is thus a priori not obvious that the scalar model is a suitable starting point for the description of fluctuations. Conversely, the influence of local randomness within the tensorial model was not yet investigated, and is very interesting *per se*. In particular, it is important to know if and how the idea of a ‘light cone’ survives in the presence of disorder, and how the stress fluctuations develop.

The aim of the present paper is to calculate analytically (in two dimensions) the average response function (Green function) and the two-point correlation function for the tensorial model in the presence of disorder, and to compare the results to those obtained within a scalar description. We find that the cone survives at small disorder (although the cone angle is shifted and acquires a non zero width, which we compute). More surprisingly, the Green function takes *negative values*¹, a feature which we checked numerically, and which we discuss in detail in terms of the essential “fragility” of the contact network. We show that the two-point correlation function keeps a signature of this cone like propagation. For large disorder however, the theory suggests that the structure of the large scale equations could change drastically, from an *hyperbolic* wave equation to an *elliptic* equation, akin to (but distinct from) those appearing in elasticity theory. The interpretation of the equations however suggests that by the time this happens, the pile is unstable to any perturbations and spontaneously rearranges.

The ‘tensorial’ stress probability distribution is investigated numerically, with certain results which are close to those of the scalar model. We explain this by showing that a special case of the tensorial model actually reduces to the superposition of *two* independent scalar models.

This paper is constructed as follows: in section 2, we review the properties of the scalar model, including results which appeared in the literature in very different contexts (scalar diffusion in turbulence, localisation). In section 3, the ‘random wave equation’ for the tensorial

¹That the Green function can take negative values in the presence of inhomogeneities was already noticed within the FPA model in [12].

case is motivated by a microscopic model and simulations, and studied using perturbation theory in the strength of the disorder. We discuss how the line shape of the response function distorts from two delta peaks to (eventually) one broad peak as disorder increases. Some generalisations of the the ‘random wave equation’ are considered in section 4. In section 5, we present numerical results for the stress distribution function and compare them with the predictions of the scalar model, and also of direct simulations of sphere packings [14, 15]. We discuss a limit where the two models can be quantitatively compared. Finally, in section 6, a summary of the most interesting results is given, with suggestions of new experiments and open questions.

2 The Scalar Model

2.1 The discrete version

- Definition.

The main assumption of the scalar model is that only the vertical normal component of the stress tensor $w = \sigma_{zz}$ (the ‘weight’) needs to be considered. If the grains reside on the

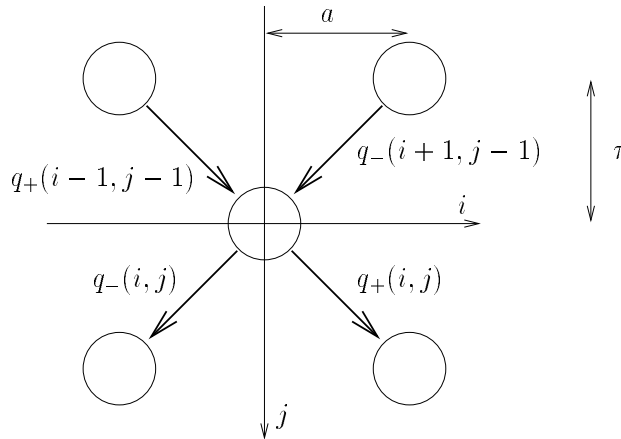


Figure 1: The ‘Chicago’ model with two neighbours. q_{\pm} ’s are independent random variables, except for the weight conservation constraint: $q_+(i, j) + q_-(i, j) = 1$.

nodes of a two-dimensional lattice (see figure 1), the simplest model for weight propagation down the pile is:

$$w(i, j) = w_g + q_+(i-1, j-1)w(i-1, j-1) + q_-(i+1, j-1)w(i+1, j-1) \quad (1)$$

where ‘ w_g ’ is the weight of each grain, and $q_{\pm}(i, j)$ are ‘transmission’ coefficients giving the fraction of weight which the grain (i, j) transmits to its right (resp. left) neighbour immediately below. Mass conservation imposes that $q_+(i, j) + q_-(i, j) = 1$ for all i, j ’s. The case of an ordered pile of identical grains would correspond to $q_{\pm} = \frac{1}{2}$. The authors of [4, 9] proposed to take into account (in a phenomenological way) the local disorder in packing, grain sizes and shapes, etc., by choosing $q_+(i, j)$ to be independent random numbers (except for the above constraint), for example uniformly distributed between 0 and 1. This model, which we shall call the ‘Chicago’ model (or q model), was originally written with an arbitrary

number N of downward neighbours ($N = 2$ in the example above), and can thus be (in principle) generalized to three dimensions.

- Results on the stress distribution. Universality ?

The case of a uniform distribution of the q 's is interesting because it leads to an exact solution for the local weight distribution $P(w)$. In this limit, the correlation between two neighbouring sites at the same altitude j is zero for all j . For more general q distributions, this is true only when j is large (see below). Thus $P(w)$ obeys the following mean-field equation:

$$P_{j+1}(w) = \int_0^1 dq_1 dq_2 \rho(q_1) \rho(q_2) \int_0^\infty dw_1 dw_2 P_j(w_1) P_j(w_2) \delta[w - (w_1 q_1 + w_2 q_2 + w_0)] \quad (2)$$

where $\rho(q)$ is the distribution of q , here taken to be $\rho(q) = 1$. In the limit $j \rightarrow \infty$, the stationary distribution P^* of this equation is given by:

$$P^*(w) = \frac{w}{W^2} \exp - \frac{w}{W} \quad (3)$$

where $2W = jw_g$ is the average weight. For $N \neq 2$, the distribution is instead a Γ distribution of parameter N ; its small w behaviour is w^{N-1} while the large w tail is exponential. Liu et al. [4, 9] have argued that this behaviour is generic: for example, the condition for the local weight w to be small is that all the N q 's reaching this site are themselves small; the phase space volume for this is proportional to w^{N-1} if the distribution $\rho(q)$ is regular around $q = 0$. However, if instead $\rho(q) \propto q^{\gamma-1}$ when q is small, one expects $P^*(w)$ to behave for small w as $w^{-\alpha}$, with $\alpha = 1 - N\gamma < 0$. Similarly, the exponential tail at large w is sensitive to the behaviour of $\rho(q)$ around $q = 1$. In particular, if the maximum value of q is $q_M < 1$, one can easily show by taking the Laplace transform of equation (2) that $P^*(w)$ decays *faster* than an exponential:

$$\log P^*(w) \underset{w \rightarrow \infty}{\propto} -w^\beta \quad \text{with} \quad \beta = \frac{\log N}{\log(Nq_M)} \quad (4)$$

(Notice that $\beta = 1$ whenever $q_M = 1$, and that $\beta \rightarrow \infty$ when $q_M = 1/N$).

In this sense, the exponential tail of $P^*(w)$ is not universal: it requires the possibility that one of the q can be arbitrarily close to 1. This implies that all other q 's originating from that point are close to zero, i.e. that there is a nonzero probability density that one grain is entirely bearing on one of its downward neighbours.

Note that if q can only take the values 0 or 1, the distribution $P(w)$ becomes a power law, $P^*(w) \propto w^{-\alpha}$, with $\alpha = 4/3$ for $N = 2$ [9]. This power law is however truncated for large w as soon as values for q different from 0 and 1 are allowed.

How well does the simple distribution (3) compare to experiments and numerical simulations? The exponential decay for large w appears in some cases to overestimate both the experimental [5] and numerical tail [15] (see also section 5), suggesting a value of β somewhat larger than 1. On the other hand, the probability to observe very small w is much underestimated by equation (3): see [5, 14, 6] and section 5. This might be due to the fact that *arching* effects are absent in this scalar model. A generalisation of the Chicago model allowing for arching was suggested in [3], which generates sites where $q_+ = 1$ and $q_- = 0$ (or vice versa). This indeed leads to much higher probability density for small weights, $P^*(w) \propto w^{-\alpha}$ as argued in [9] – see also [16].

2.2 Continuous limit of the scalar model.

Let us focus on the case $N = 2$ and define v to be such that $q_{\pm}(i, j) = (1 \pm v(i, j))/2$. If v is small, the local weight is smoothly varying, and the discrete equation (1) can then be written in the following differential form:

$$\partial_t w + \partial_x(vw) = \rho + D_0 \partial_{xx} w \quad (5)$$

where $x = ia$ and $t = j\tau$ are the horizontal and (downwards) vertical variables corresponding to indices i and j of figure 1, and a and τ are of the order of the size of the grains. The vertical coordinate has been called t for its obvious analogy with time in a diffusion problem. ρ is the density of the material (the gravity g is taken to be equal to 1), and D_0 a ‘diffusion’ constant, which depends on the geometry of the lattice on which the discrete model has been defined. For a rectangular lattice as shown in figure 1, $D_0 = \frac{a^2}{2\tau}$. More generally, the diffusion constant is of the order of magnitude of the size of the grains, a .

In this model and in the following, we shall assume that the density ρ is not fluctuating. Density fluctuations could be easily included; it is however easy to understand that the resulting relative fluctuations of the weight at the bottom of the pile decrease with the height of the pile H as $H^{-1/2}$, and are thus much smaller than those induced by the randomly fluctuating direction of propagation, encoded by q (or v), which remain of order 1 as $H \rightarrow \infty$.

Two interesting quantities to compute are the average ‘response’ $G(x, t|x_0, t_0)$ to a small density change at point (x_0, t_0) , measured at point (x, t) , and the correlation function of the force field, $C(x, t, x', t') = \langle w(x, t)w(x', t') \rangle_c$ (connected part), where the averaging is taken over the realisation of the noise $v(x, t)$.

Equation (5) shows that the scalar model of stress propagation is identical to that describing tracer diffusion in a (time dependent) flow $v(x, t)$. This problem has been the subject of many recent works in the context of turbulence [17, 18]; we believe that interesting qualitative analogies with that field can be made. In particular, ‘intermittent’ bunching of the tracer field correspond in the present context to patches of large stresses, which may induce anomalous scaling for higher moments of the stress field correlation function. We refer the reader to [17, 18] for further details.

- Statistics of the noise $v(x, t)$.

The noise term v represents the effect of local heterogeneities in the granular packing. Its mean value is taken to be zero, and its correlation function is chosen for simplicity to be of the factorable form $\langle v(x, t)v(x', t') \rangle = \sigma^2 g_x(x - x')g_t(t - t')$, where g_x and g_t are noise correlation functions along x and t axis. We shall take g_x and g_t to be short-ranged (although this may not be justified: fluctuations in the microstructure of granular media may turn out to be long-ranged due to e.g. the presence of long stress paths or arches), with correlation lengths ℓ_x and ℓ_t . Our aim is to describe the system at a scale L much larger than both the lattice and the correlation lengths: $a, \tau, \ell_x, \ell_t \ll L$. This will allow us to look for solutions in the regime $k, E \rightarrow 0$, where k and E are the conjugate variables for x and t respectively, in Fourier-Laplace space. However, we shall see below that the limit $a, \tau, \ell_x, \ell_t \rightarrow 0$ can be tricky, and must be treated with care: this is because the noise appears in a multiplicative manner in equation (5)². For computational purposes, we shall often implicitly assume that the probability distribution of v is gaussian; this might however introduce artefacts which we discuss.

²In the tensorial case, the limit $\ell_t \rightarrow 0$ actually makes the problem trivial, for a reason which will become clear below.

- Fourier transforms.

The limit where $a, \ell_x \rightarrow 0$ is ill defined and leads to a divergence of the perturbation theory in σ for large wavevectors k . We thus choose to regularize the problem by working within the first Brillouin zone, i.e., we keep all wave vector components within the interval $\mathcal{I} = [-\Lambda, +\Lambda]$, where $\Lambda = \frac{\pi}{a}$. Our Fourier conventions for a given quantity f will then be the following:

$$f(x, t) = \int_{-\Lambda}^{\Lambda} \frac{dk}{2\pi} e^{ikx} f(k, t) \quad (6)$$

$$f(k, t) = \ell_x \sum_{x=-\infty}^{+\infty} e^{-ikx} f(x, t) \quad (7)$$

One has to be particularly careful when computing convolution integrals, such as $\int \frac{dq}{2\pi} f_1(q) f_2(k-q)$ which must be understood with limits $-\Lambda + k, \Lambda$ (resp. $-\Lambda, \Lambda + k$) if $k \geq 0$ (resp. $k \leq 0$). An important example, which will appear in the response function calculations, is:

$$\int_{q, k-q \in \mathcal{I}} \frac{dq}{2\pi} q = \frac{\Lambda k}{2\pi} + \mathcal{O}(k^2) \quad (8)$$

Let us then take the Fourier transform of equation (5) along x , to obtain:

$$(\partial_t + D_0 k^2) w_k = \rho_k + ik \int \frac{dq}{2\pi} w_q v_{k-q} \quad (9)$$

Our aim is to calculate, in the small- k limit, the average response (or Green) function $G(k, t-t')$ defined as the expectation value of the functional derivative $\langle \delta w(k, t) / \delta \rho(k, t') \rangle$; and the two points correlation function of w , $\langle w(k, t) w(k', t) \rangle \equiv 2\pi \delta(k+k') C(k, t)$.

- The noiseless Green function.

The noiseless (bare) Green function (or ‘propagator’) G_0 is the solution of the equation where the ‘velocity’ components v_q are identically zero: $(\partial_t + D_0 k^2) G_0(k, t-t') = \delta(t-t')$ which is:

$$G_0(k, t-t') = \theta(t-t') e^{-D_0 k^2 (t-t')} \quad (10)$$

Or, in real space,

$$G_0(x, t-t') = \frac{\theta(t-t')}{\sqrt{4\pi D_0 (t-t')}} e^{-\frac{x^2}{4D_0 (t-t')}} \quad (11)$$

- Ambiguities due to multiplicative noise. Ito vs. Stratonovitch.

In equation (9), we have omitted to specify the dependence on the variable t . There is actually an ambiguity in the product term $w_q v_{k-q}$. In the discrete Chicago model [4], the q_{\pm} ’s emitted from a given site are independent of the value of the weight on that site. In the continuum limit, this corresponds to choosing $w_q(t)$ to be independent of $v_{k-q}(t)$, or else that the v ’s must be thought of as slightly posterior to the w ’s (i.e. the product is read as $w_q(t-0) v_{k-q}(t+0)$). In this case, the average of equation (9) is trivial and coincides with the noiseless limit; hence $G = G_0$. This can be understood directly on the discrete model by noticing that the Green function $G(i, j|0, 0)$ can be expressed as a sum over paths, all starting at site $(0, 0)$, and ending at site (i, j) :

$$G(i, j|0, 0) = \sum_{\text{paths } \mathcal{P}} \prod_{(k, l) \in \mathcal{P}} q_{\pm}(k, l) \quad (12)$$

where the $q_{\pm}(k, l)$ are either $q_+(k, l)$ or $q_-(k, l)$, depending on the path. Since each bond $q_{\pm}(k, l)$ appears only once in the product, the averaging over q is trivial and leads to:

$$G(i, j|0, 0) = \sum_{\text{paths } \mathcal{P}} 2^{-j} \equiv G_0(i, j|0, 0) \quad (13)$$

(Note that this argument fails for the computation of the correlation function C , since paths can ‘interfere’. We shall return later to this calculation.)

The above choice corresponds to Ito’s prescription in stochastic calculus. Another choice (i.e. Stratonovitch’s prescription) is however possible, which corresponds to the proper continuum time limit in the case where the correlation length ℓ_t is very small, but not smaller than a (see figure 2). In this case, the w ’s and the v ’s cannot be taken to be independent. This is the choice that we shall make in the following.

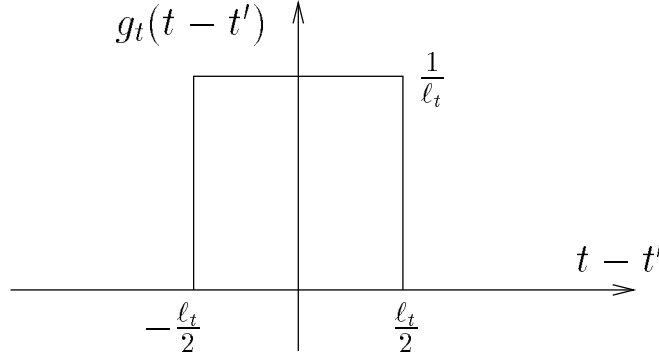


Figure 2: Correlation function of the noise along t axis. The results presented below would hold for an arbitrary symmetric, short range function.

2.3 Calculation of the averaged response and correlation functions.

Two approaches will be presented. The first one, based on Novikov’s theorem, leads to exact differential equations for G and C , which can be fully solved. The second one is a mode-coupling approximation (MCA), based on a resummation of perturbation theory. It happens that, for this particular model where the noise is gaussian and short range correlated in time, both approaches give the same results, because perturbation theory is trivial. In other cases, though, where exact solutions are no longer available, the MCA is in general very useful to obtain non perturbative results (see [22]).

We shall see that the effect of the noise is to widen the diffusion peak: D_0 is renormalized by an additional term proportional to the variance of the noise v .

- Novikov’s theorem. Exact equations for G .

Novikov’s theorem provides the following identity, valid if the v are gaussian random variables:

$$\langle w(k, t)v(k', t) \rangle = \int_0^t dt' \int dq \left\langle \frac{\delta w(k, t)}{\delta v(q, t')} \right\rangle \langle v(q, t')v(k', t) \rangle \quad (14)$$

Such a term actually appears in equation (9), after transformation into an equation for G :

$$(\partial_t + D_0 k^2)G(k, t - t') = \delta(t - t') - ik \frac{\delta}{\delta \rho(k, t')} \int \frac{dq}{2\pi} \langle v(q, t)w(k - q, t) \rangle \quad (15)$$

In the limit where $\ell_x = a \rightarrow 0$, the noise correlation is of the form: $\langle v(q, t)v(q', t') \rangle = 2\pi\sigma^2\delta(q + q')\tilde{g}_x(q)g_t(t - t')$, with g_t peaked in $t = t'$ such that $f(t')g_t(t - t') \simeq f(t)g_t(t - t')$ for any function f . In all section 2 we take $g_x(q) = 1$. From formally integrating equation (9) between t' and t , one can express the equal-time derivative $\delta w/\delta v$ as:

$$\left. \frac{\delta w(k, t)}{\delta v(k', t')} \right|_{t'=t-0} = -ikw(k - k', t) \quad (16)$$

and thus obtain:

$$(\partial_t + D_0 k^2)G(k, t - t') = \delta(t - t') - 2\pi\sigma^2 k G(k, t - t') \int_0^t dt' g_t(t - t') \int \frac{dq}{2\pi} (k - q) \quad (17)$$

Using the shape of the function g_t (see figure 2), the first integral is $1/2$. The second one is a convolution integral, and its value is $\Lambda k/2\pi + \mathcal{O}(k^2)$ (see equation (8)). The final differential equation for G is then, in the small- k limit, a diffusion equation with a renormalized diffusion constant:

$$D_R = D_0 + \frac{\sigma^2 \Lambda}{2} \quad (18)$$

It is interesting to note that the model remains well defined in the limit where the ‘bare’ diffusion constant is zero, since a non zero diffusion constant is induced by the fluctuating velocity v . This would not be true if equation (5) was interpreted with the Ito convention, where the fluctuating velocity would *not* lead to any spreading of the average density.

The most important conclusion is thus that, in the present scalar model, stresses propagates essentially vertically: taking $\ell \sim a$, the response at depth H to a small perturbation is confined within a distance $\propto \sqrt{D_R H}$ from the vertical. Since $D_R \simeq \ell^2/a$, $\sqrt{D_R H}$ is much less than H in the limit where $H \gg \ell^2/a$, i.e. when the height of the assembly of grains is much larger than the grain size.

- Exact equations for C .

Exact equations can also be derived for C , following very similar calculations. From equation (9), one can deduce the corresponding one for $w(k, t)w(-k, t)$. Upon averaging, Novikov’s theorem has to be used on quantities such as $\langle w(k, t)v(q, t)w(-k - q, t) \rangle$, finally leading to:

$$(\partial_t + 2D_R k^2)C(k, t) = \sigma^2 k^2 \int \frac{dq}{2\pi} C(q, t) \quad (19)$$

One can formally integrate equation (19). It gives

$$C(k, t) = C(k, 0)e^{-2D_R k^2 t} + \sigma^2 k^2 \int_0^t dt' e^{-2D_R k^2 (t-t')} \tilde{C}(t') \quad (20)$$

where $\tilde{C}(t') = \int \frac{dk}{2\pi} C(k, t')$. Let us specify at this stage two specific initial conditions $C(k, 0)$ which can be of interest. We consider, for simplicity, a random packing of ‘table tennis’ balls with no mass ($\rho = 0$), but subject to a random overload of zero mean ($\langle w(x, 0)w(x', 0) \rangle = A_0^2 \delta(x - x')$) or to a constant overload ($w(x, t = 0) = B_0$). Therefore, $C(k, 0) = A_0^2$ in the first case, and $C(k, 0) = B_0^2 \delta(k)$ in the second one. Equation (20) is then solved in two steps: we first integrate it over k and find a closed equation for \tilde{C} , which can be solved in Laplace transform. We call E the conjugate variable of t . From $\tilde{C}(E)$, we get $\tilde{C}(t)$ and then finally compute $C(x, t)$.

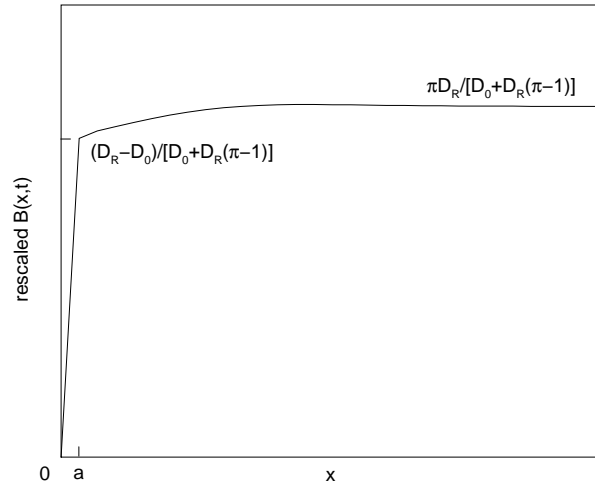


Figure 3: Correlation function for the case of a random overload. B has been rescaled by the factor $\frac{A_0^2}{[8\pi D_R t]^{1/2}}$.

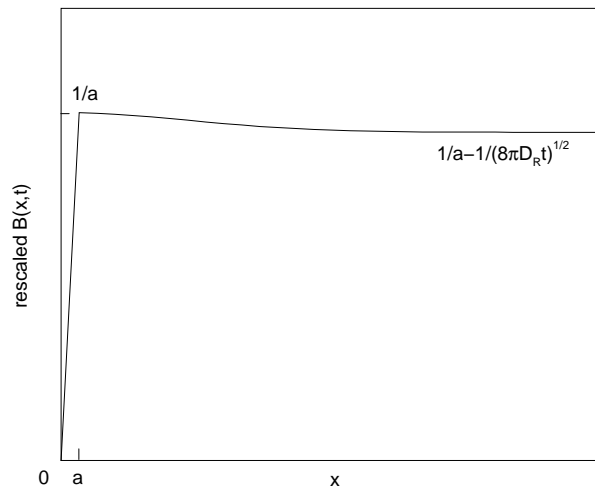


Figure 4: Correlation function for the case of a uniform overload. B has been rescaled by the factor $\frac{\sigma^2 B_0^2}{4[D_0 + D_R(\pi - 1)]}$.

◦ Random overload: in the small E (large t) limit, we get $\tilde{C}(E) \sim 1/\sqrt{E}$, meaning $\tilde{C}(t) = a_0/\sqrt{t}$, with $a_0 = \frac{\pi D_R}{D_0 + D_R(\pi - 1)} \frac{A_0}{\sqrt{8\pi D_R}}$. It finally leads to the following expression for $B(x, t) \equiv C(0, t) - C(x, t) = 1/2 \langle [w(x, t) - w(0, t)]^2 \rangle$:

$$B(x = 0, t) = 0$$

$$B(x \gg a, t) = \frac{A_0^2}{\sqrt{8\pi D_R t}} \left[1 - e^{-\frac{x^2}{8D_R t}} + \frac{\pi\sigma^2}{2[D_0 + D_R(\pi - 1)]} \left(\frac{1}{a} + \frac{x}{8D_R t} e^{-\frac{x^2}{8D_R t}} \right) \right] \quad (21)$$

which is shown in figure 3.

◦ Constant overload: in the same limit, we get $\tilde{C}(E) \sim 1/E$, or $\tilde{C}(t) = b_0$, where $b_0 = B_0^2 \frac{D_R}{2[D_0 + D_R(\pi - 1)]}$. Hence:

$$B(x = 0, t) = 0$$

$$B(x \neq 0, t) = \frac{\sigma^2 B_0^2}{4[D_0 + D_R(\pi - 1)]} \left[\frac{1}{a} - \frac{1 - e^{-\frac{x^2}{8D_R t}}}{\sqrt{8\pi D_R t}} \right] \quad (22)$$

which has a form similar to that above: see figure 4.

One could have performed the calculation with the Ito convention (corresponding to the Chicago model). The final results for the correlation function are actually very similar to those above. The main point is that the correlation is rather structureless. Equation (22) shows that the correlation function $C(x > a, t)$ becomes zero for large times, a result that was used to establish equation (2).

- Perturbation theory.

The above method gives exact results, essentially because $v(x, t)$ is short range correlated in time: $\delta w/\delta v$ is then only needed at coinciding times, where it is exactly known. This would not be true in general; furthermore Novikov's theorem requires v to be gaussian. It is thus interesting to show how a systematic perturbation scheme can be made to work by the use of diagrams to represent equation (9). The MCA (Mode Coupling Approximation) is then a particular resummation scheme of this set of diagrams, which was discussed in detail in [22], which sometimes provide interesting non perturbative results.

Equation (9) is multiplied on the left by the operator G_0 (see equation (10)), and then reexpressed as follows:

$$w(k, t) = G_0(k, t) \otimes \rho(k, t) - ikG_0(k, t) \otimes \int \frac{dq}{2\pi} w(q, t) v(k - q, t) \quad (23)$$

\otimes meaning a t -convolution product. This equation can be represented with diagrams as follows: as shown in figure 5, we represent the source ρ by a cross, the 'bare' propagator G_0 by a plain line and the noise v by a dashed line. The first term of equation (23), which is the noiseless solution w_0 , is then obtained the juxtaposition of a plain line and a cross. The arrow flows against time (i.e. it is directed from t to $t' < t$). The juxtaposition of two objects means a t -convolution product. By definition w is represented by the juxtaposition of a bold line and a cross (this is consistent with the identification of a bold line with the full propagator G). The diagrammatic version of equation (23) is then:

$\xrightarrow{\text{bold } k} \times = \xrightarrow{\text{plain } k} \times + \xrightarrow{\text{plain } k} \text{---} \xrightarrow{\text{dashed } k-q} \times$

(24)

$$\begin{aligned}
\rho(k, t) &= \times & G_0(k, t) &= \xrightarrow{k} & w_0(k, t) &= \xrightarrow{k} \times \\
v(k, t) &= \text{---} \xrightarrow{k} \text{---} & G(k, t) &= \xrightarrow{k} & w(k, t) &= \xrightarrow{k} \times \\
\langle v^2 \rangle &= \text{---} \xrightarrow{\quad} \text{---} \circ \text{---} \xleftarrow{\quad} \text{---} & \Sigma(k, t - t') &= \xrightarrow{k-q} \text{---} \xrightarrow{q} \text{---} \xrightarrow{q-k} \text{---}
\end{aligned}$$

Figure 5: definition of various diagrams.

The ‘vertex’ stands for $-ik \int \frac{dq}{2\pi}$, the two emerging wave vectors being q and $k - q$ (node law). One can now iterate this equation. To second order, one obtains:

$$\xrightarrow{k} \times = \xrightarrow{k} \times + \xrightarrow{k} \text{---} \uparrow \text{---} \times + \xrightarrow{k} \text{---} \uparrow \text{---} \uparrow \text{---} \times \quad (25)$$

The corresponding equation for G is obtained by taking the derivative $\delta/\delta\rho$, and averaging over the noise v . Since $\langle v \rangle = 0$, the second diagram vanishes. We represent the noise correlator by a dashed line with a centered circle (see figure 5), and obtain:

$$\xrightarrow{k} = \xrightarrow{k} + \xrightarrow{k} \text{---} \text{---} \circ \text{---} \text{---} \xrightarrow{k} \quad (26)$$

or $G = G_0 + G_0 \Sigma G_0$, where Σ is called the self-energy (see figure 5). Actually, one can resum exactly all the diagrams corresponding to $G_0 \Sigma G_0$, $G_0 \Sigma G_0 \Sigma G_0$ to obtain the Dyson equation $G = G_0 + G_0 \Sigma G$.

The MCA amounts to replacing the ‘bare’ propagator in the diagram for Σ by the full propagator G . (Note that the MCA is of course exact to second order in perturbation theory). We then obtain a self-consistent equation for G :

$$\Sigma_{\text{MCA}} = G_0^{-1} - G_{\text{MCA}}^{-1} = \xrightarrow{k} \text{---} \text{---} \circ \text{---} \text{---} \xrightarrow{k} \quad (27)$$

Diagrams like the one drawn in figure 6 are now also included. The self-energy Σ_{MCA} can be

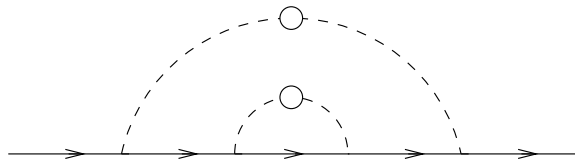


Figure 6: Example of a diagram included in the MCA.

easily computed, we get

$$\Sigma_{\text{MCA}}(k, t - t') = -2\pi\sigma^2 k \int \frac{dq}{2\pi} q G_{\text{MCA}}(q, t - t') g_t(t - t') \quad (28)$$

In the special case where g_t is peaked around $t = t'$, we can make the approximation $G(q, t - t')g_t(t - t') \simeq G(q, 0)g_t(t - t') = g_t(t - t')$ (since by definition $G(q, 0) = 1$). We thus get, using equation (8), $\Sigma_{\text{MCA}}(k, t - t') = -\sigma^2\Lambda k^2 g_t(t - t')$. The expression for G_{MCA}^{-1} is thus identical to the one obtained with the exact approach, as can be seen by comparing equation (17) and $G_0^{-1}G = 1 + \Sigma G$.

Note that one can also calculate the influence of a non zero kurtosis κ of the noise v , which is its normalized fourth cumulant. In this case, four dashed lines (corresponding to v) can be merged, leading to a contribution to D , of the order of $\kappa\sigma^4$.

Let us turn now to the calculation of the correlation function $\langle w(k, t)w(k', t) \rangle \equiv 2\pi\delta(k + k')C(k, t)$. The basic object which corresponds to the self-energy is now the 'renormalized source' spectrum $S(k, t, t')$ defined as: $C = G \otimes S \otimes G$. The quantity S is drawn as a filled square. S_0 (empty square) is the correlation function source term which encodes the initial conditions (see below). The two first terms of the expansion are

$$\blacksquare = \square + \text{loop diagram} + \dots \quad (29)$$

Here again, we transform the perturbative expansion into a closed self-consistent equation for S by replacing G_0 and S_0 in (29) by G and S respectively. The final equation for C reads:

$$\text{arrow-filled square} = \text{arrow-empty square} + \text{arrow-loop diagram} \quad (30)$$

or, written explicitly,

$$C(k, t) = \int_0^t dt' \int_0^t dt'' G(k, t - t') S_0(k, t', t'') G(-k, t - t'') + \sigma^2 k^2 \int_0^t dt' \int_0^t dt'' G(k, t - t') \int \frac{dq}{2\pi} C(q, t', t'') g_t(t' - t'') G(-k, t - t'') \quad (31)$$

If we choose the source term to be an overload localised at $t = 0$, we get: $S_0 = \langle \rho(k, t')\rho(-k, t'') \rangle = C(k, 0)\delta(t')\delta(t'')$.

Using the fact that g_t is peaked around $t' = t''$, we again recover exactly the equation (19) above, showing again that MCA is exact in this special case.

2.4 Further results: the unaveraged response function

The *average* Green function described above is thus a Gaussian of zero mean, and of width growing as $\sqrt{D_R t}$. However, for a *given* environment, the Green function is not Gaussian, presenting sample dependent peaks (see figure 7). Note however that, contrarily to what we shall find below for the tensorial case, the unaveraged Green function remains everywhere positive. Furthermore, the quantity $[x](t)$, defined as the displacement of the centroid of the weight distribution beneath a point source in a given realisation:

$$[x](t) = \int_{-\infty}^{+\infty} dx' x' \frac{\delta w(x', t)}{\delta \rho(0, 0)} \quad (32)$$

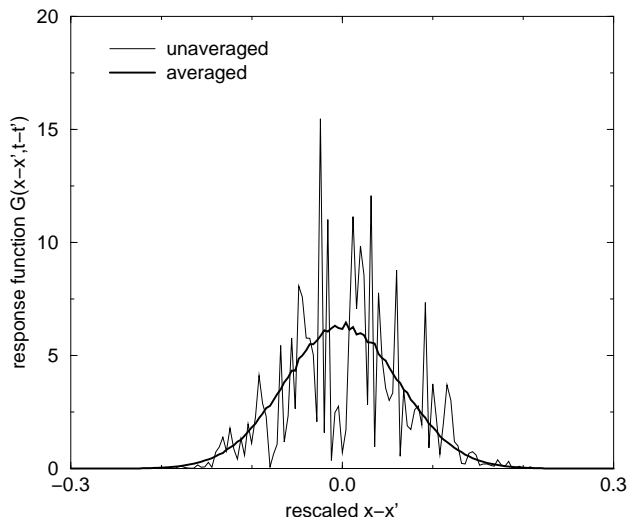


Figure 7: Averaged (bold line) and unaveraged (thin line) response function of the scalar model, obtained numerically by simulating the Chicago model. The average is performed over 5000 samples. One can notice how ‘non self averaging’ is the response function, i.e. how different it is for a given environment as compared to the average. Note also that the unaveraged Green function is everywhere positive.

typically grows with t . More precisely, one can show that:

$$\langle [x](t) \rangle = 0 \quad \text{but} \quad \langle [x]^2(t) \rangle \propto t^{1/2} \quad (33)$$

meaning that the ‘center’ of Green function wanders away from the origin in a subdiffusive fashion, as $t^{1/4}$. This behaviour has actually been obtained in an another context, that of a quantum particle interacting with a time dependent random environment. Physically, the Chicago model can indeed be seen as a collection of time dependent scatterers, converting ingoing waves into outgoing waves with a certain partition factor $q_+ = 1 - q_-$ (see the discussion in [19]). In two dimensions (plus time), the wandering of the packet center $[x](t)$ is only logarithmic (and disappears in higher dimensions [19]).

2.5 The scalar model with bias: Edwards’ picture of arches

Up to now, we have considered the mean value of v to be zero, which reflects the fact that there is no preferred direction for stress propagation. In some cases however, this may not be true. Consider for example a sandpile built from a point source: the history of the grains will certainly imprint a certain oriented ‘texture’ to the contact network, which can be modelled, within the present scalar model, as a non zero value of $\langle v \rangle$, the sign of which depends on which side of the pile is chosen. Let us call V_0 the average value of v on the $x \geq 0$ side of the pile, and $-V_0$ on the other side. The differential equation describing propagation now reads, in the absence of disorder:

$$\partial_t w + \partial_x [V_0 \text{sign}(x)w] = \rho + D_0 \partial_{xx} w \quad (34)$$

(An extra noise can be handled as above). For a constant density $\rho = \rho_0$, and for $D_0 = 0$,

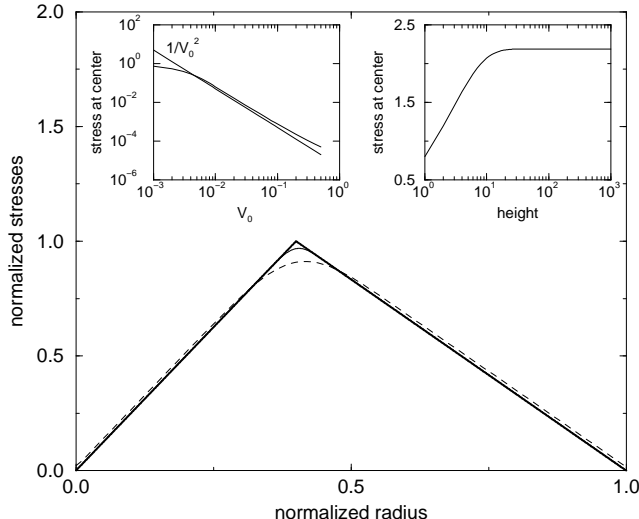


Figure 8: On the main graph is plotted the solution of equation (34) for $V_0/c = 0.4$. The dashed line is for a diffusion constant D_0 ten times smaller than the the solid one. The bold line is for $D_0 = 0$. Stress values are rescaled by the height of the pile t . The left inset graph shows that $w(0, t)$ scales like $1/V_0^2$ at small V_0 while the right inset shows that $w(0, t)$ is constant for large t . Note that for very small values of V_0 , the $1/V_0^2$ scaling becomes invalid for finite size reasons.

the weight distribution is then the following:

$$\begin{aligned}
 w(x, t) &= \frac{\rho_0 x}{V_0} & \text{for } 0 \leq x \leq V_0 t \\
 w(x, t) &= \frac{\rho_0 (ct - x)}{c - V_0} & \text{for } V_0 t \leq x \leq ct
 \end{aligned} \tag{35}$$

where $c = 1/\tan(\phi)$ (ϕ is the angle made by the slope of the pile with the horizontal x axis). For $D_0 \neq 0$, the above solution is smoothed (see figure 8). In any case, the local weight reaches a *minimum* around $x = 0$. Equation (34) gives a precise mathematical content to Edwards' model of arching in sandpiles [20], as the physical mechanism leading to a 'dip' in the pressure distribution [21]. As discussed elsewhere [11, 12], this can be taken much further within a tensorial framework (see section 3).

The scaling of the stress at the center of the pile, $w(0, t)$, can be understood simply in terms of random walks subject to a bias V_0 . The region contributing to $w(0, t)$ is then found to be of finite volume, independent of t , and of the order of D_0/V_0^2 , as shown on the two top pictures of figure 8.

Equation (34) with noise can in fact be obtained naturally within an extended Chicago model, with an extra rule accounting for the fact that a grain can slide and lose contact with one of its two downward neighbours [3]. This generically leads to arching; in the sandpile geometry and for above a certain probability of (local) sliding, the effective 'velocity' V_0 becomes non zero and the weight profile (35) is recovered [3]. However, this extra sliding rule implicitly refers to the existence of shear stresses, which are absent in the scalar model, but which are crucial to obtain symmetry breaking effects modelled by a non zero V_0 . It is thus important to consider from the start the fact that stress has a tensorial, rather than scalar, nature. This is what we investigate in the following section.

3 The Tensorial Model

3.1 The wave equation

It is useful to start with a simple ‘toy’ model for stress propagation, which is the analogue of the model presented in figure 1. We now consider the case of three downward neighbours (see figure 9), for a reason which will become clear below. Each grain transmits to its downward

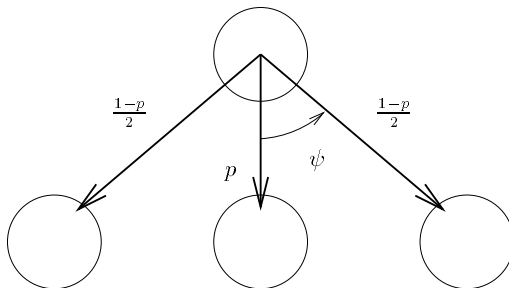


Figure 9: Three neighbour configuration. Each grain transmits two force components to its downward neighbours. A fraction p of the vertical component is transmitted through the middle leg, and a fraction $(1 - p)/2$ through each of the external legs.

neighbours not one, but two force components: one along the vertical axis t and one along x , which we call respectively $F_t(i, j)$ and $F_x(i, j)$. (We will restrict attention, in the sequel, to two-dimensional piles, leaving extensions to three dimensions for further investigations.) For simplicity, we assume that the ‘legs’ emerging from a given grain can only transport the vector component of the force parallel to itself (but more general rules could be invented). Assuming that the transmission rules are locally symmetric, and that a fraction $p \leq 1$ of the vertical component travels through the middle leg, we find:

$$F_x(i, j) = \frac{1}{2} [F_x(i - 1, j - 1) + F_x(i + 1, j - 1)] + \frac{1}{2}(1 - p) \tan \psi [F_t(i - 1, j - 1) - F_t(i + 1, j - 1)] \quad (36)$$

$$F_t(i, j) = w_0 + pF_t(i, j - 1) + \frac{1}{2}(1 - p) [F_t(i - 1, j - 1) + F_t(i + 1, j - 1)] + \frac{1}{2 \tan \psi} [F_x(i - 1, j - 1) - F_x(i + 1, j - 1)] \quad (37)$$

where ψ is the angle between grains, defined in figure 9. Taking the continuum limit of the above equations leads to:

$$\partial_t F_t + \partial_x F_x = \rho \quad (38)$$

$$\partial_t F_x + \partial_x [c_0^2 F_t] = 0 \quad (39)$$

where $c_0^2 \equiv (1 - p) \tan^2 \psi$. Eliminating (say) F_x between the above two equations leads to a *wave equation* for F_t , where the vertical coordinate t plays the rôle of time and c_0 is the equivalent of the ‘speed of light’. In particular, the stress does not propagate vertically, as it does in the scalar model, but rather at a *non zero angle* φ such that $c_0 = \tan \varphi$. Note that $\varphi \neq \psi$ in general (unless $p = 0$); the angle at which stress propagates has nothing to do with the underlying lattice structure and can in principle be arbitrary. We chose a three leg model to illustrate this particular point.

The above derivation can be reformulated in terms of classical continuum mechanics as follows. Considering all stress tensor components σ_{ij} , the equilibrium equation reads,

$$\partial_t \sigma_{tt} + \partial_x \sigma_{xt} = \rho \quad (40)$$

$$\partial_t \sigma_{tx} + \partial_x \sigma_{xx} = 0 \quad (41)$$

Identifying the local average of F_t with σ_{tt} and that of F_x with σ_{tx} , we see that the above equations (38, 39) are actually identical to (40, 41) provided $\sigma_{tx} = \sigma_{xt}$ (which corresponds to the absence of local torque) and $\sigma_{xx} = c_0^2 \sigma_{tt}$. This relation between normal stresses was postulated in [10] as the simplest constitutive relation obeying the correct symmetries which enables one to lift the indeterminacy of equations (40, 41); it can be seen as a *local* Janssen approximation [13]. c_0^2 should encode the relevant information of the local geometry of the packing, friction, shape of grains, etc., and should thus depend on the construction history of the grain assembly. For example, in the sandpile geometry c_0^2 is related to the angle of friction ϕ of the material by the relation $c_0^2 = 1/(1 + 2 \tan^2 \phi)$ [10]. This approach can be generalized to take into account a local asymmetry in the packing texture (which one expects for example in the case of a sandpile constructed from a point source), by allowing c_0^2 to depend on σ_{xt}/σ_{tt} [10, 11, 12]. If this dependence is linear, this is equivalent to a coordinate rotation in x, t [12].

3.2 A stochastic wave equation

The starting point of the scalar model is thus essentially the diffusion equation, which one perturbs by adding a random convective term. As the above paragraph shows, a more natural starting point is the wave equation. The toy model presented above however suggests that, provided local conservation laws are obeyed (i.e. those arising from mechanical equilibrium), many local rules for force transmission are compatible with the contact conditions [15]. It is thus natural to encode the disorder of the packing, or model the indeterminacy of the contact conditions as a randomly varying ‘speed of light’ c_0 (reflecting the fact that, for example, the parameter p can vary from grain to grain). Two recent numerical simulations [15, 23] actually suggest that this should be a good first approximation. In figure 10, we show a scatter plot of σ_{xx} versus σ_{tt} , measured as averages of the local forces over a small box centered around different points within a heap (from ref.[23]). This plot clearly shows that a linear relation is indeed acceptable, leading in this case to $c_0^2 \sim 0.56 \pm 0.03$ [23]. There are however significant fluctuations, reflecting some disorder in the packing, which are furthermore uncorrelated from point to point. The histogram of v defined as:

$$\sigma_{xx} = c_0^2 [1 + v(x, t)] \sigma_{tt} \quad \langle v(x, t) \rangle = 0 \quad (42)$$

is found to be roughly gaussian, of relative width $\sigma \sim 0.3$. This corresponds to a locally varying angle of stress propagation, which varies around the mean angle 54° by an amount $\sim 10.8^\circ$.

Motivated by the simulations results, we now investigate a model (called ‘random symmetric model’ in the following) with the inhomogeneous constitutive relation (42), which leads to the following stochastic wave equation for stress propagation:

$$\partial_{tt} \sigma_{tt} = \partial_{xx} \left[c_0^2 (1 + v(x, t)) \sigma_{tt} \right] \quad (43)$$

where the random noise v is assumed to be correlated as $\langle v(x, t) v(x', t') \rangle = \sigma^2 g_x(x - x') g_t(t - t')$. The correlation lengths ℓ_x and ℓ_t are again kept finite, and of the same order of magnitude. In Fourier transform, this relation can also be written $\langle v(k, t) v(k', t') \rangle = 2\pi \sigma^2 \delta(k + k') \tilde{g}_x(k) g_t(t - t')$. It turns out that the final shape of the averaged response function depends

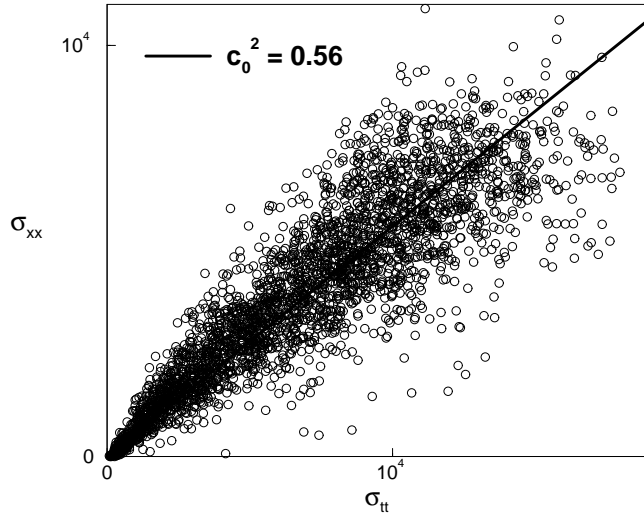


Figure 10: Relation between σ_{xx} and σ_{tt} from a microscopic numerical simulation of grains forming a heap in two dimensions [23]. These data are compatible with a stochastic constitutive relation $\sigma_{xx} = c_0^2[1 + v(x, t)]\sigma_{tt}$, where v is a random noise.

on the sign of $\tilde{g}_x(\Lambda)$. In section 2 we implicitly made the choice $\tilde{g}_x(k) = 1$, which corresponds to: $g_x(x = 0) = 1/a$ and $g_x(x > 0) = 0$. We will keep this choice for the following calculations, but note that another form for g_x could lead to $\text{sign}(\tilde{g}_x(\Lambda)) = -1$.

In the following, σ_{tt} will be again denoted by w . After a Fourier transform along x -axis, we get, from equation (43)

$$(\partial_{tt} + c_0^2 k^2)w = \partial_t \rho - c_0^2 k^2 \int \frac{dq}{2\pi} w(q, t) v(k - q, t) \quad (44)$$

Note that the ‘source’ term of this equation is now $\partial_t \rho$ rather than ρ itself. Therefore, if we call G the Green function (or propagator) of this equation $G = \langle \delta w / \delta \partial_t \rho \rangle$; the response function $R = \langle \delta w / \delta \rho \rangle$ of our system is now actually the time derivative of G : $R(k, t) = \partial_t G(k, t)$.

The noiseless propagator G_0 is the solution of the ordinary wave equation $(\partial_{tt} + c_0^2 k^2)G_0(k, t - t') = \delta(t - t')$ and can be easily calculated:

$$G_0(k, t) = \frac{1}{2ic_0 k} \left[e^{ic_0 k t} - e^{-ic_0 k t} \right] \theta(t) \quad (45)$$

which leads to the response function R_0

$$R_0(x, t) = \frac{1}{2} [\delta(x - c_0 t) + \delta(x + c_0 t)] \theta(t) \quad (46)$$

This last equation sums up one of the major results of [10] (see also [11, 12]): in two dimensions, stress propagates along two characteristic rays. (Note that the corresponding response function in three dimensions³ reads $R_0(x, t) \propto (c_0^2 t^2 - x^2)^{-1/2}$ for $|x| < c_0 t$ and zero otherwise [10]). A relevant question is now to ask how these rays survive in the presence of disorder. We will show that for weak disorder, the δ -peaks acquire a finite (diffusive) width, and that

³In three dimensions a secondary closure is needed, for instance $\sigma_{xx} = \sigma_{yy}$, y being the third coordinate.

the ‘speed of light’ is renormalized to a lower value. Not surprisingly, the effect of disorder can be described by an ‘optical index’ $n > 1$. For a strong disorder, however, we find (within a gaussian approximation for the noise v) that the speed of light vanishes and then becomes imaginary. The ‘propagative’ nature of the stress transmission disappears and the system behaves more like an elastic body, in a sense clarified below.

3.3 Calculation of the averaged response function

One can again use Novikov’s theorem in the present case if the noise is gaussian and short range correlated in time. However, the same results are again obtained within the diagrammatic approach explained in section 2, which can be easily transposed to the present case, and is more general. The propagator G is now represented as a line, the source $\partial_t \rho$ a cross and the vertex meaning $-c_0^2 k^2 \int \frac{dq}{2\pi}$. Within the MCA, the self-consistent equation (analogous to equation (27) in the scalar case) is:

$$(\partial_{tt} + c_0^2 k^2)H(k, t) = \delta(t) + \int_0^t dt' \Sigma_{\text{MCA}}(k, t')H(k, t - t') \quad (47)$$

where H is defined by $G(k, t) = H(k, t)\theta(t)$, and the self-energy Σ_{MCA} given as

$$\Sigma_{\text{MCA}}(k, t - t') = 2\pi c_0^4 \sigma^2 k^2 \int \frac{dq}{2\pi} q^2 g_t(t - t') \tilde{g}_x(k - q)H(q, t - t') \quad (48)$$

Equation (47) can be solved using a standard Laplace transform along the t -axis (E is the Laplace variable). Using the fact that $H(k, \tau) = \tau$ in the limit where $\tau \rightarrow 0$, we find, for small k, E (corresponding to scales L such that $\ell_x, \ell_t \ll L$): $H^{-1}(k, E) = E^2 + \beta E + c_R^2 k^2$, where

$$c_R^2(k) = c_0^2 - \frac{c_0^4 \sigma^2 \Lambda^3 \ell_t}{6} \left(1 - \frac{3|k|}{2\Lambda}\right) + \mathcal{O}(k^2) \quad (49)$$

$$\beta(k) = \frac{c_0^4 \sigma^2 k^2 \Lambda^3 \ell_t^2}{9} + \mathcal{O}(k^3) \quad (50)$$

We notice here that in the limit $\ell_t \rightarrow 0$, the effect of the randomness completely disappears, as in the scalar model with the Ito convention. (Technically, this is due to the fact that $G(k, t = 0) \equiv 0$ in the present problem). In order to calculate the inverse Laplace transform, we need to know the roots of the equation $H^{-1}(k, E) = 0$. This leads to several phases, depending on the strength of the disorder.

- The weak disorder limit.

For a weak disorder, $c_R^2(k)$ is always positive. We can then define $c_R = c_R(k = 0)$. As we will show now, c_R is the shifted ‘cone’ angle along which stress propagates asymptotically. c_R is a decreasing function of σ , meaning that the peaks of the response function get closer together as the disorder increases⁴. For a critical value⁵ $\sigma = \sigma_c$, c_R vanishes, and becomes imaginary for stronger disorder.

In the limit of large t , the propagator reads:

$$G(k, t) = \frac{1}{c_R k} \sin [c_R k t (1 + \alpha |k|)] e^{-\gamma k^2 t} \theta(t) \quad (51)$$

⁴As a technical remark, let us note that if $g_t = g_x$, the problem is symmetric in the change $x \rightarrow t$, $c_0^2(x, t) \rightarrow 1/c_0^2(x, t)$. It thus looks as if the cone should both narrow or widen, depending on the arbitrary choice of x and t . There is however no contradiction with the above calculation since we assumed that v has zero mean, while $1/(1 + v) - 1$ has a positive mean value, of order σ^2 .

⁵For $\ell_t = \ell_x = 1$ and $c_0^2 = 0.6$ (corresponding to $\phi = 30^\circ$), one finds $\sigma_c \simeq 0.57$.

where the following constants have been introduced ⁶:

$$\alpha = \frac{3}{4\Lambda} \left(\frac{c_0^2}{c_R^2} - 1 \right) \quad (52)$$

$$\gamma = \frac{\beta(k)}{2k^2} = \frac{\sigma^2 \Lambda^3 \ell_t^2}{18} \quad (53)$$

From equation (51), the response function R , in the limit of small k and large t , is given by:

$$R(k, t) = \cos [c_R k t (1 + \alpha |k|)] e^{-\gamma k^2 t} \theta(t) \quad (54)$$

or in real space,

$$R(x, t) = \frac{1}{2\sqrt{4\pi|\hat{\gamma}|t}} \Re \left\{ \frac{e^{-\xi_+^2/b}}{\sqrt{b}} \left[1 - \Phi\left(-i\frac{\xi_+}{\sqrt{b}}\right) \right] + \sqrt{b} e^{-b\xi_-^2} \left[1 - \Phi(-i\sqrt{b}\xi_-) \right] \right\} \quad (55)$$

where the scaling variables ξ_{\pm} , measuring distances relative to the two peaks, are defined by

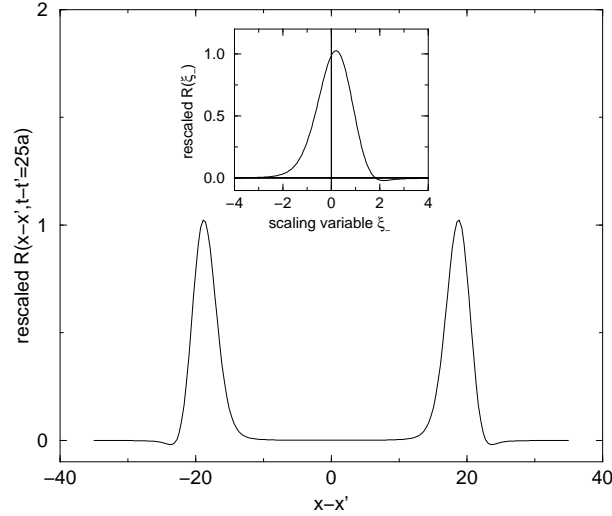


Figure 11: Response function for weak disorder ($\sigma/\sigma_c \sim 0.32$). The two curves have been rescaled by the factor $2[4\pi|\hat{\gamma}|t]^{1/2}$. The main graph shows the general double-peaked shape of the response of the system when subjected to a peaked overload at $x = 0$, $t = 0$. The inset gives details the right-hand peak as a function of the scaling variable ξ_- . Note the asymmetry (for $\tilde{g}_x(\Lambda) > 0$), compatible with the results found in [15]. Note also that the curve becomes negative around $\xi_- = 2$.

$$\xi_{\pm} = \frac{x \pm c_R t}{\sqrt{4|\hat{\gamma}|t}} \quad (56)$$

and where $\hat{\gamma} = \gamma - ic_R \alpha$ and $b = e^{i \arg \hat{\gamma}}$. Φ is the standard error function. Figure 11 shows R as given by expression (55). Interestingly, this propagator not only has a finite diffusive width $\propto \sqrt{t}$, but is also asymmetric around its maxima. Surprisingly, and in sharp contrast to the scalar case discussed above, the response function becomes *negative* in certain intervals

⁶Note that the sign of α is dictated by the sign of $\tilde{g}_x(\Lambda)$.

(although its integral is of course equal to one because of weight conservation). This means that pushing on a given point actually reduces the downward pressure on certain points. This can be interpreted as some kind of arching: increasing the shear stress does affect the propagation of the vertical stress, and may indeed lead to a reduction in its local value which is redistributed elsewhere. As we shall see in section 5, the unaveraged response function indeed takes negative (and rather large) values. This is a very significant result since it suggests that granular materials may be susceptible to rearrangement under extremely weak external perturbations. Suppose indeed that as a result of the perturbation, a grain receives to a negative force larger than the preexisting vertical pressure. This grain will then move and a local rearrangement of contacts will occur, inducing a variation of $c_0(x, t)$ as to reduce the cause of the instability. Thus, the stochastic wave equation implicitly demands rules similar to those introduced in [3] to describe extreme sensitivity to external perturbations in silos. The present model, which is purely static, does not say what to do when a local rearrangement occurs, but certainly suggests that small perturbations will induce such rearrangements.

It is interesting to note that this response function was numerically measured in ref. [15]; its shape is compatible with the above expression; in particular, the two peaks were found to be asymmetric with a longer ‘tail’ extending inwards, as we obtain here. Note however that for $\tilde{g}_x(\Lambda) < 0$, the shape of the peaks is reversed: the small dips are located inside the peaks and the longer tail extends outwards. This is actually what we obtain numerically in section 5.

- Shear response function.

Equation (40) provides a straightforward way to calculate the shear response function R_s in terms of R . Indeed, one has: $ikR_s(k, t) = \delta(t) - \partial_t R(k, t)$. We thus get, in the limit of small k and large t ,

$$R_s(k, t) = -ic_R \sin [c_R kt(1 + \alpha|k|)] e^{-\gamma k^2 t} \theta(t) \quad (57)$$

This shear response function is very similar to R , except that it is, as expected, an odd function of x .

- Effective large scale equations.

It is interesting to know of which differential equations the response functions R and R_s , are solutions. These effective equations can be interpreted as a coarse-grained (hydrodynamical) description of the propagation of a stress perturbation which takes into account the average effect of the local disorder. One problem however comes from the presence of the ‘dispersion’ term $\alpha|k|$, which corresponds to a non-local operator in real space. We thus neglect this term in the following discussion, but one should keep in mind that the effective equation are actually non local. In any case, the main features of the response functions (peaks centered around $x = \pm c_R t$ ($c_R < c_0$) with a diffusive width $\propto \sqrt{t}$) are not lost when setting $\alpha = 0$ (except for the fact that the response function can become negative which is related to $\alpha \neq 0$). Effective equations can then be written in the large t limit as:

$$\partial_t \langle \delta \sigma_{tt} \rangle = \delta \rho - \partial_x \langle \delta \sigma_{xt} \rangle \quad (58)$$

$$\partial_t \langle \delta \sigma_{xt} \rangle = -c_R^2 \partial_x \langle \delta \sigma_{tt} \rangle + 2\gamma \partial_{xx} \langle \delta \sigma_{xt} \rangle \quad (59)$$

That disorder generates the diffusion terms $2\gamma \partial_{xx} \langle \delta \sigma_{xt} \rangle$ is rather intuitive and had been guessed in [10]. This terms can be seen the first term of a gradient expansion of to the constitutive equations which have the correct symmetry, i.e.:

$$\langle \delta \sigma_{xx} \rangle = c_R^2 \langle \delta \sigma_{tt} \rangle - \gamma \partial_x \langle \delta \sigma_{xt} \rangle \quad (60)$$

$$\langle \delta\sigma_{tx} \rangle = \langle \delta\sigma_{xt} \rangle \quad (61)$$

where the second equation is imposed by the absence of local torque.

We have thus shown that the introduction of a small disorder in the local direction of propagation does not change radically the nature of stress propagation on large length scales, although the peaks in the response function acquire a diffusive width. These peaks acquire a width of the order of $\sqrt{\gamma H}$ (where H is the height of the pile), and are thus well separated in the limit where $H \gg \gamma$. As we shall see now, this is no longer true if the disorder becomes strong.

- Critical disorder: The wave/diffusion transition.

When the disorder is so strong that c_R just vanishes, the roots of $H^{-1}(k, E) = 0$ change nature, and so does the response function R . The two peaks of the previous expression for R merge together, while the width becomes anomalously large ($\propto t^{2/3}$). In the asymptotic, large t , regime we obtain:

$$R(k, t) = \theta(t) \cos \left[\lambda |k|^{3/2} t \right] e^{-\gamma k^2 t} \quad (62)$$

where the new constant λ is defined by $\lambda = c_0 \sqrt{3/2\Lambda}$ and $\gamma = c_0^2 \ell_t / 3$. The physical response

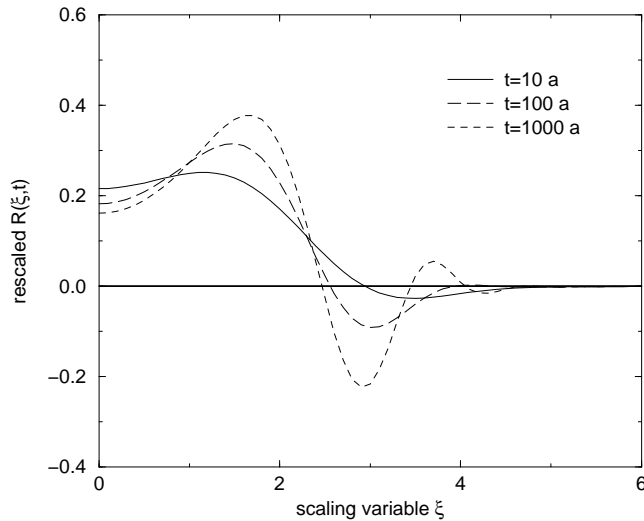


Figure 12: Response function for a critical disorder: $c_R = 0$.

function R is plotted in figure 12, for different values of t , as a function of the scaling variable

$$\xi = \frac{x}{\lambda t^{2/3}}. \quad (63)$$

On the scale $t^{2/3}$, the double peak structure of R is still visible. However, note that the term $e^{-\gamma k^2 t}$ cannot be neglected, even for large t ; this means that the response function is never really a function of ξ only, as clear from figure 12. Note that the response function again becomes negative for some values of ξ .

- Strong disorder: The pseudoelastic regime.

For larger disorder still, one finds, within the MCA (which is exact for a gaussian, uncorrelated noise), that the renormalized value of c_0^2 , c_R^2 , becomes negative. Upon a rescaling of x as $\hat{x} = x/(ic_R)$, the effective equation on $\langle \delta\sigma_{tt} \rangle$ then becomes, on large length scales, Poisson's equation:

$$\nabla^2 \langle \delta\sigma_{tt} \rangle = \partial_t \langle \delta\rho \rangle \quad (64)$$

which means that the stress propagation becomes somewhat similar to that in an elastic body, where stresses obey an elliptic equation of similar type [24]. In particular, the cone structure of stress propagation, which is associated with the underlying, hyperbolic, wave equation finally disappears; the average response to a localised perturbation becomes a broad 'bump' of width comparable to the height of the pile. It is thus rather interesting to see that, within MCA, there is a phase transition from a 'wavelike' mode to a 'diffusive' mode of stress propagation; the observation of the 'cone' thus requires that the packing is not too disordered. Certainly for relatively ordered packings the cone exists and has been observed experimentally [25] and numerically [15]. One should however add some remarks:

– It is possible that the above transition is an artefact, due to the fact that v is taken to be gaussian, which strictly speaking is not allowed, since the local value of c_0^2 should always be positive. One can show for some other problems of the same type that a similar transition is artificially induced by the gaussian approximation when it cannot really exist on physical grounds. In this respect, it is interesting to note that the first non gaussian correction tends to increase c_R , for negative kurtosis as might be expected for a bounded v distribution.

– It should be noted that the predicted effective constitutive relation between horizontal and vertical normal stresses has a negative sign if $c_R^2 < 0$. This means that increasing the vertical stress should reduce the horizontal stress, which is only possible if the grains move. Hence, the region where $c_R^2 < 0$ is probably impossible to reach physically: the system will rearrange spontaneously as to reduce the disorder, and to make $c_R^2 \geq 0$. Note however that, as already discussed above, the disorder which results of such a rearrangement might be strongly correlated, and correspond to an arching effect, as in [3].

3.4 The correlation function

Coming back to the weak disorder case, the major problem for the direct observation of the 'light cone' is the fact that the perturbation representing the point source should be small (otherwise the packing structure would change in an inhomogeneous way, thereby affecting the value of c_0^2 in a non uniform way), but large enough for the response to be detected. A better possibility, as we show now, could be to measure the correlation function of the stress field. We again consider the stress correlation function in the case where the mass of each grain is small ($\rho = 0$) and a random or a constant overload is applied on the top of the 'silo'. With the new convention for the bar (for G) and the cross (for $\partial_t\rho$), the self-consistent diagrammatic equation (30) is strictly valid in the tensorial case. When writing it into its usual mathematical form, the only difference with the scalar model is that now the weight source term is $w(k, 0)\delta'(t)$, leading to $S_0(k, t', t'') = C(k, 0)\delta'(t')\delta'(t'')$.

The calculation of the correlation function is very similar to the scalar case. In order to carry out the calculations to the end, we have neglected the dispersion term $\alpha|k|$ in the expressions for G and R . The analogue of equation (20) is now, for weak disorder,

$$C(k, t) = C(k, 0) \cos^2 [c_R k t] e^{-2\gamma k^2 t} + \sigma^2 \frac{c_0^4}{c_R^2} k^2 \int_0^t dt' \sin^2 [c_R k (t - t')] e^{-2\gamma k^2 (t-t')} \tilde{C}(t') \quad (65)$$

The function $\tilde{C}(t') = \int \frac{dk}{2\pi} C(k, t')$ is of identical form to the scalar case; only the expressions for a_0 (for the random overload) and b_0 (for the constant overload) are different:

$$a_0 = \frac{A_0^2}{4\sqrt{2\pi\gamma}} \cdot \frac{1}{1 - \frac{\sigma^2 c_0^4}{4\pi\gamma^2 c_R^2} \arctan\left(\frac{\pi\gamma}{c_R}\right)} \quad (66)$$

$$b_0 = \frac{B_0^2}{2\pi} \cdot \frac{1}{1 - \frac{\sigma^2 c_0^4}{4\pi\gamma^2 c_R^2} \arctan\left(\frac{\pi\gamma}{c_R}\right)} \quad (67)$$

Knowing $\tilde{C}(t')$, $C(x, t)$ can be computed from equation (65). For the case of a constant overload, the shape of the correlation function is very close to the one showed in figure 4 for the scalar model. The case of the random overload however is much more interesting since the fact that information travels along a cone of angle c_R appears clearly: the correlation function presents *two* peaks. The first one is of course at $x = 0$, while the second is at $x = 2c_R t$, which simply means that the two points at the bottom of the information cone share the same information coming from the apex of this cone ⁷. If we forget the second term of the right

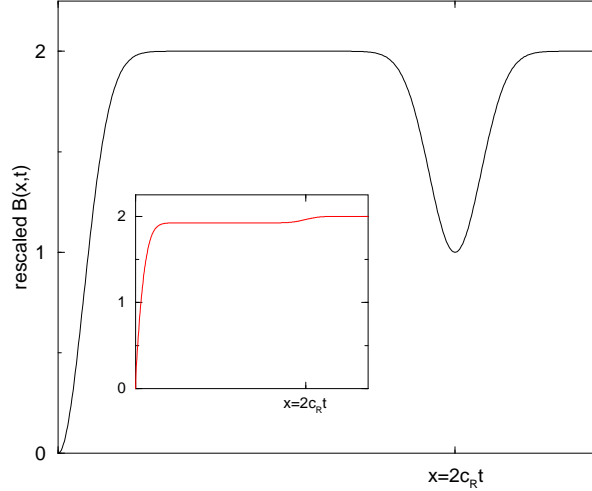


Figure 13: Correlation function for the case of a random overload. Note the presence of a peak centered in $x = 2c_R t$ which reflects the fact that information in the tensorial model is travelling along a cone of angle of c_R . In the case of a fluctuating density in the bulk of the pile, one should integrate (68) with respect to t . The result is plotted in the inset: the correlation reaches rapidly a first plateau, and then increases again to a higher value around $x = 2c_R t$. The relative difference of height between the two plateaus decreases as $t^{-1/2}$.

hand of equation (65) which is negligible compared to the first one at large t , we can see that the second peak of the correlation function has a width $\propto \sqrt{t}$ and a height $\propto 1/\sqrt{t}$. This approximation is actually equivalent to saying that the (linear) effective equations (58, 59) are sufficient to calculate the correlation function for large times. Other source terms, such as a fluctuating density in the bulk of the pile, can thus be easily accommodated by linear

⁷In the absence of disorder, the correlation function consists of two δ peaks, one at $x = 0$ and the other at $x = 2c_0 t$ of half the amplitude.

superposition. We have thus plotted on figure 13 the quantity $B(x, t) = C(0, t) - C(x, t)$, omitting the second term in the r.h.s. of equation (65). Analytically, we have

$$B(x, t) = \frac{A_0^2}{4\sqrt{8\pi\gamma t}} \left[2 + 2e^{-\frac{c_R^2 t}{2\gamma}} - 2e^{-\frac{x^2}{8\gamma t}} - e^{-\frac{(x+2c_R t)^2}{8\gamma t}} - e^{-\frac{(x-2c_R t)^2}{8\gamma t}} \right] \quad (68)$$

This result is of importance since the shape of this correlation function clearly differs from the corresponding one in the scalar model. Measuring carefully the averaged correlation function of a granular system could then confirm (or disprove) the presence of a light ray-like propagation. In this respect, it is interesting to plot the correlation function for three dimensional packings as well. This correlation function only depends on the radial distance r between the

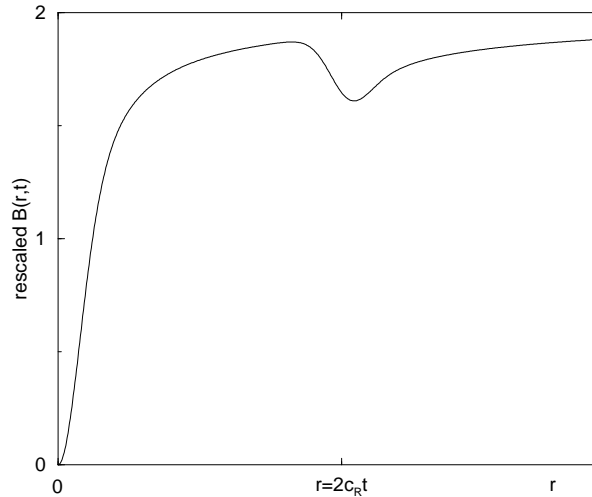


Figure 14: Correlation function for three dimensional disordered packings with a random overload, neglecting again the second term in equation (65). Note that, as in two dimensions, the correlation function exhibits a peak around $r = 2c_R t$.

two points, as is plotted in figure 14. We note that, much as in two dimensions, the correlation decreases sharply on the scale of a few grains, but increases again for distances of the order of the height of the pile. Note that a stress correlation function was actually recently measured in [6] and found to be featureless, but on very short scales $x \leq 5a$, as compared to the height of the pile $H \simeq 100a$. We thus expect the features of the correlation function to show up on much larger scales $\sim 2c_R H$.

4 Generalized wave equations

It is tempting to generalize equations (38, 39) and write the most general linear equations governing the propagation of the forces which are compatible with the (local) conservation rules. These equations were first written by de Gennes [26]:

$$\partial_t F_t + \partial_x [\eta'(x, t) F_x + \mu'(x, t) F_t] = \rho \quad (69)$$

$$\partial_t F_x + \partial_x [\eta(x, t) F_t + \mu(x, t) F_x] = 0 \quad (70)$$

Note that the terms μ, μ' break the symmetry $x \rightarrow -x$. This is allowed locally and does not show up on large scales if their average is zero. Another possibility (but without noise), considered in detail in [12], is that $\mu(x, t)$ changes sign with x , i.e.: $\mu(x, t) = \mu \text{sign}(x)$, which describes the fact that the texture of a sandpile depends on which ‘side’ of the pile one is looking at. Interestingly, equations (69, 70) still lead to wave-like propagation, but now the bisector of the ‘light cone’ makes a non zero angle with the vertical (when μ or μ' are non zero). In other words, equations (69, 70) describe a situation where not only the opening angle of the cone can vary in space, but also its average orientation.

The same analytical techniques as above can be still be used. We shall only discuss some special cases ⁸:

◦ Let us first set $\mu = \mu' = 0$ and consider the case where η' is random, and η fixed (and equal to c_0^2). Taking $\eta'(x, t) = \eta'_0 (1 + v(x, t))$ with the noise v as above, one finds that the renormalized value of η' is:

$$\eta'_R = \eta'_0 \left(1 - \frac{c_0^2 \eta'_0 \sigma^2 \Lambda^3 \ell_t}{6} \right) \quad (71)$$

Now, on large length scales, one must recover the continuum equilibrium equations for the stress tensor, equations (40, 41). The condition of zero torque requires that the stress tensor is symmetric, and thus one must set $\eta'_R \equiv 1$, which imposes a relation between η'_0 and the amplitude of the noise σ . Note that beyond a certain value of σ , this relation can no longer be satisfied with a real η'_0 . This again means that the packing is unstable mechanically and will rearrange so as to reduce the disorder.

◦ Another interesting class of models, which one can call ‘ μ models’, is such that: $\eta = c_0^2, \eta' = 1$, but $\mu(x, t) = c_0 v(x, t)$ and $\mu' = 0$ or vice-versa. These two cases yield identical results, namely, in the large t limit:

$$R(k, t) = \cos(c_0 k t) e^{-\gamma k^2 t} \theta(t) \quad (72)$$

$$R_s(k, t) = -i c_0 \sin(c_0 k t) e^{-\gamma k^2 t} \theta(t) \quad (73)$$

where $\gamma = \frac{c_0^2 \Lambda \sigma^2}{4}$. Note that in these cases, the response peaks acquire a finite diffusive width $\propto \sqrt{t}$, but the angle of the information cone is unaffected by the disorder (i.e. c_0 is not renormalized).

◦ Finally, there are special ‘symmetry’ conditions where the equations can be decoupled and reduced to two ‘scalar’ models. We will refer to this case as the ‘double scalar’ model. This occurs when $\mu = \mu' = c_0 v_1(x, t)$ and $\eta' = \eta/c_0^2 = 1 + v_2(x, t)$ where v_1, v_2 are two different sets of noise. Let us define $\sigma_{\pm} = c_0 F_t \pm F_x$, $x_{\pm} = x \mp c_0 t$ and $v_{\pm} = v_1 \pm v_2$, we then obtain:

$$\partial_t \sigma_+ = c_0 \rho - c_0 \partial_{x_+} [v_+ \sigma_+] \quad (74)$$

$$\partial_t \sigma_- = c_0 \rho - c_0 \partial_{x_-} [v_- \sigma_-] \quad (75)$$

showing that σ_+ and σ_- decouple, each propagating along two rays, of ‘velocity’ $\pm c_0$, plus a small noise v_{\pm} which, as in the scalar case, generates a nonzero diffusion constant. The response functions for σ_{tt} and σ_{xt} are thus again made of two diffusive peaks of width $\propto \sqrt{t}$, centered in $x = \pm c_0 t$. The interest of this double scalar limit is that one can deduce simply the probability distribution of the stresses from the Chicago model. This is developed below. Note also that by construction, this special form of disorder does not lead to negative vertical stresses.

⁸To lowest order in perturbation theory, the case where disorder is present in the four terms η, η', μ, μ' simultaneously is very simply obtained by adding the corrections induced by each term taken individually.

5 Stress distribution within the tensorial model

A physically relevant question is to know how local stresses are distributed. We have seen above that within a scalar approach, an exponential-like distribution (possibly of the type $\exp -w^\beta$, with $\beta \geq 1$) is expected [4, 9]. One can wonder whether this exponential distribution survives within a tensorial description, and what happens for very small stresses $w \rightarrow 0$. Unfortunately, the full distribution can only be computed analytically for the ‘double scalar’ model; but numerical results have also been obtained for the random symmetric model, and are described below.

5.1 The ‘double-scalar’ limit

In the ‘double scalar’ limit, the histogram of the stress distribution is obtained trivially by noting that since $\sigma_+ = w_1$ and $\sigma_- = w_2$ travel along different paths, they are independent random variables. Taking c_0 to be unity for simplicity, one thus finds:

$$P(\sigma_{tt}) = \int dw_1 \int dw_2 P^*(w_1) P^*(w_2) \delta(\sigma_{tt} - \frac{w_1 + w_2}{2}) \quad (76)$$

$$P(\sigma_{xt}) = \int dw_1 \int dw_2 P^*(w_1) P^*(w_2) \delta(\sigma_{xt} - \frac{w_1 - w_2}{2}) \quad (77)$$

where P^* is the distribution of weight pertaining to the scalar case, which, as mentioned above, depends on the specific form of the local disorder and on the discretisation procedure. In the strong disorder case which leads to equation (3) [in the case $N = 2$], we thus find that $P(\sigma_{tt})$ is still decaying exponentially (it is actually a Γ distribution of parameter $2N$), although its variance is reduced by a factor 2. For $N = 2$, one simply gets

$$P(\sigma_{tt}) = \frac{8}{3} \sigma_{tt}^3 e^{-2\sigma_{tt}} \quad (78)$$

$$P(\sigma_{xt}) = \left(|\sigma_{xt}| + \frac{1}{2} \right) e^{-2|\sigma_{xt}|} \quad (79)$$

The preexponential factor is therefore noticeable different from the prediction of equation (3).

5.2 Numerical histograms for the random symmetric model and open problems

The numerical analysis of equations (40, 41), with a stochastic constitutive relation $\sigma_{xx} = \eta[1 + v(x, t)]\sigma_{tt}$ is actually not an easy task, and the final results depend rather sensitively on the chosen discretisation. For example, a naive discretisation of the random wave equation leads to a non zero diffusive width even in the absence of disorder, and thus makes it hard to measure the ‘true’ response function, which should, in the absence of disorder, consists of two δ peaks. However, it should be noted that such diffusive term (or order a) are actually expected physically – they indeed appear when equations (36, 37) are expanded to second order in the lattice spacing. We shall come back to this point below.

The method we chose is the following. Starting with points regularly arranged at $t = 0$, we construct the network of characteristics (in the mathematical sense). To each point (x, t) is associated a ‘speed of light’ $c_0(x, t) = c_0 \sqrt{[1 + v(x, t)]}$ which determines the directions of lines which propagate the component of the stress parallel to that line, away from the point (x, t) . The point (x, t) is then generated by two ‘parents’ points (x', t') and (x'', t'') as indicated on figure 15-(a). It sometimes happens that the cone from (x', t') is so wide that it cannot intersect with the one from (x'', t'') [see figure 15-(b)]. We then impose $x = x''$ and $t = t''$.

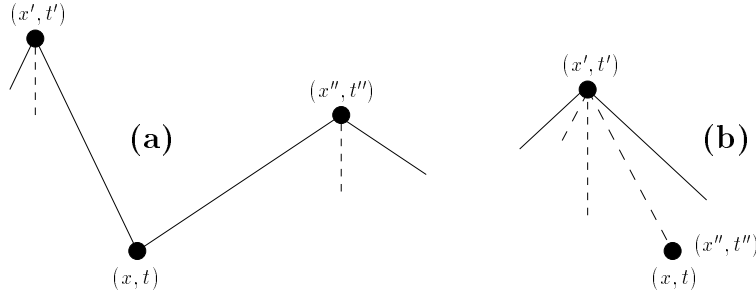


Figure 15: The left-hand picture (a) shows the construction rule of the characteristics network: the ‘child’ point (x, t) is located at the intersection of the cones from the two ‘parent’ points (x', t') and (x'', t'') . When the cones do not intersect (b), we choose (x, t) and (x'', t'') to be coincident.

This actually can be viewed as a local kind of arching: the point (x'', t'') not only supports its ‘parent’ neighbours but also its ‘same generation’ neighbour (x', t') . This method has several advantages. Its physical interpretation is very clear: points are ‘grains’ and characteristics are ‘stress paths’. Figure 16 shows an example of the network of those paths. We can see how stress paths actually merge together and generate arching. Furthermore, there is strictly no diffusion in the absence of disorder, i.e. the Green function is exactly given by the sum of two δ -peaks.

Although the noise v has been implicitly considered to be gaussian throughout this paper, for numerical simplicity we chose the following algorithm for the calculation of $v(x, t)$. At each site (x, t) , a random angle θ is uniformly chosen between $-\Delta\frac{\pi}{4}$ and $\Delta\frac{\pi}{4}$. Δ controls the amplitude of the noise. We then set $c_0(x, t) = c_0 \tan(\pi/4 + \theta(x, t))$; v and θ are then related by $v(x, t) = \frac{4 \tan \theta(x, t)}{(1 - \tan \theta(x, t))^2}$. However, since the lattice itself is generated by the disorder, the precise correlation function g_x of the v ’s is not well controlled in this numerical scheme. This is rather important since we showed in section 3 that the structure of g_x influences the shape of the response function (it determines whether the negative part of the response lies on the inward or outside edge of the main peak). In fact, the structure of the peaks we obtain numerically is reversed compared to that of our analytical calculation: see figure 17.

The numerical histogram of the force distribution at the bottom of a ‘silo’ computed within this numerical scheme immediately reveals some problems. Since the lattice becomes more distorted as ‘time’ grows, the numerical histogram of vertical forces keeps broadening and never reaches a stationary shape. Furthermore, there is a nonzero probability of observing *negative* weights which is, as we pointed out already, a structural property of the wave equation with randomness. Clearly, from a physical point of view, this is unacceptable and an additional rule should be added if the weight becomes locally negative. Some physically motivated rules could be invented (much as in [3]), but we do not want to pursue this here, and leave this for future investigations.

In the present paper, we restrict to the case of a nonzero ‘bare’ diffusion constant which, as argued above, should exist on a physical basis. Numerically, we have implemented this in two different ways.

- The first one corresponds to letting the above scheme run until some height t_D and then start afresh with a regular lattice, where the forces are obtained by averaging over the nearest neighbours belonging to the ‘old’ lattice. This averaging procedure is clearly equivalent to a diffusion term. In this case, the numerical histograms do reach a stationary limit. We note that:

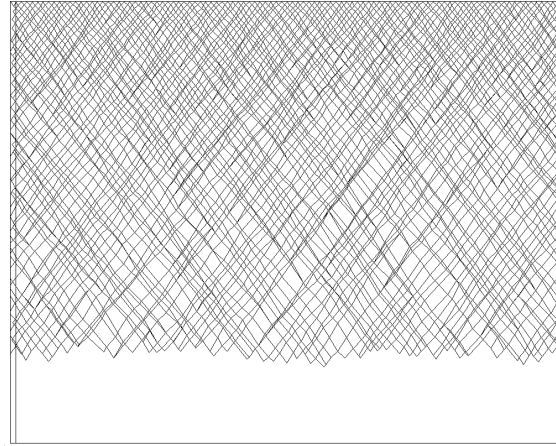


Figure 16: Stress path network for a periodic silo of width $100 a$. This picture has been computed with $\Delta = 0.2$. We have chosen periodic lateral boundary conditions.

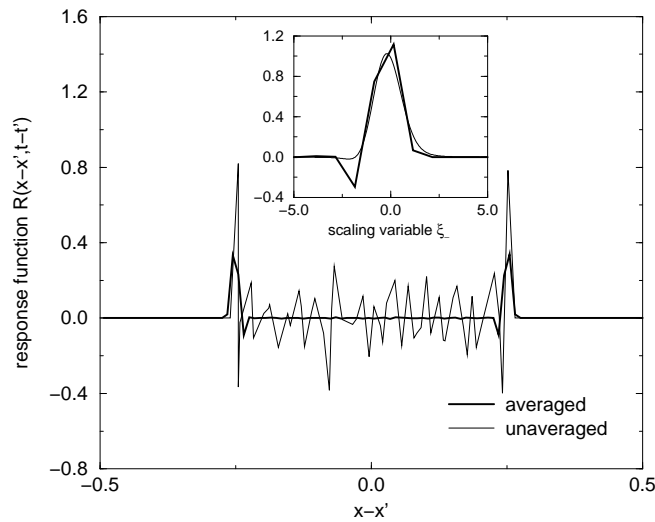


Figure 17: The main graph shows the response function calculated numerically on a silo of width $100 a$ with $\Delta = 0.2$. The thin line is a typical response for a given realisation of the disorder. Note that it takes negative values. The bold line has been averaged over 5000 realisation of the disorder. The inset compares the averaged response peak with the one computed analytically, with a negative α . Note the negative part, as predicted by the theoretical calculation.

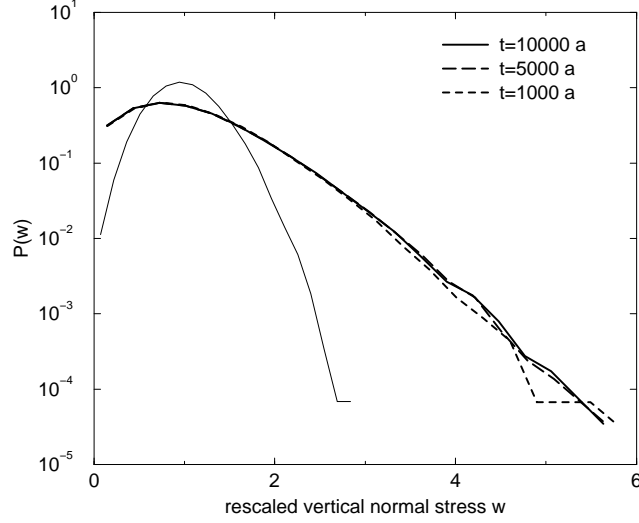


Figure 18: These curves show the histograms of the vertical normal stress w , from which negative values have been removed. They all have been computed for the three-leg model, with periodic ‘silos’ of width $1000 a$. The three bold (solid, long-dashed and dashed) lines are results from silos where the amplitude of the noise is maximum ($p_M = 1$). The height of those silos is as indicated in the legends. On the contrary, the thin line represent a $1000 a \times 1000 a$ silo where the amplitude of the noise is $p_M = 0.5$ where it is nearly gaussian. Much like within the scalar model, $P(w)$ shows an exponential tail for large values of w when the disorder is maximum, while it is better fitted by a stretched exponential, $\log P(w) \sim -w^\beta$ with $\beta > 1$, for smaller values of p_M .

- The total probability of negative forces is reduced when t_D is smaller.
- For $t_D \sim a$, the histogram is very nearly gaussian around the average force.
- For larger t_D , the tail of the probability distribution for large forces is of the form $\exp -w^\beta$, where $2 > \beta > 1$ (as found in [15]), where β is decreasing towards one as t_D increases, or for increasing disorder. For $t_D = 10 a$ and $\Delta = 0.1$, we found $\beta \simeq 1.6$. The small force region has a much larger weight than found within the scalar model, although the presence of negative forces prevents us from being conclusive in this region.

◦ The second scheme consists in simulating directly the three-leg model introduced above, with a random p chosen between 0 and p_M . These scheme is thus very close in spirit to the Chicago model. Again, the local forces are not everywhere positive, and thus the small force region cannot be reliably studied. Nevertheless, the large force region, however, behaves much in the same way as in the Chicago model. In particular, as shown in figure 18, the tail of the distribution decays as $\exp -w^\beta$, with $\beta \simeq 1$ when $p_M = 1$, and with $\beta > 1$ when $p_M < 1$.

More work is needed to understand the physical implications of the presence of negative forces and any relation this may have to the static avalanche phenomenon [3]. However, the above results show that the tail of the force distribution is only exponential in a ‘strong disorder’ limit, where local ‘arches’ (i.e. one grain entirely bearing on a single downward neighbour) has a non zero probability.

6 Summary-Conclusion

We have investigated in great detail the rôle of a local disorder in the propagation of stresses in granular media, both within a ‘scalar’ approach, where only one component of the stress tensor is retained, and within the full tensorial approach, using a simple linear closure scheme (called ‘BCC’ in [11, 12]), motivated partly by numerical simulations, which leads to a wave-like equation for stress propagation. The main effect of this local disorder is, besides introducing a diffusion like term in the effective, large scale equations, to renormalise the opening of the angle of the characteristic ‘light cone’ for propagation of stress. Within a ‘Mode-Coupling’ approximation (MCA) scheme (exact for uncorrelated gaussian noise), one finds that this angle vanishes for a critical disorder, beyond which stress propagates in a fundamentally different way (this regime might however not be physically relevant). The most striking difference between the scalar and tensorial approach, is the fact that the response function becomes negative in the latter case, which is a source of instability of the packing to external perturbations. For moderate disorder, the response function takes negative values of order one near the point where the perturbation is applied, and decays with distance. Hence, we expect this instability to occur near the point where the perturbation is applied; at least near the upper surface of a pile under gravity, the effect occurs for a stress perturbation as small as the weight of one grain, since this is sufficient to make the total local vertical stress negative !

Another difference which could be amenable to experimental verification is the structure of the correlation function, which gives direct information on how the information travels in the medium. Because of the analogy between the scalar model and passive scalar convection in turbulence, it is furthermore possible that higher moments of the correlation functions might reveal, in some circumstances, an intermittent behaviour. Finally, the exponential fall off of the local stress distribution at high values, first found within the scalar model, also holds within a tensorial approach, but requires large disorder.

Several open points remain for further studies. First of all, we have only considered two dimensional packings. The extension to three dimensions is rather straightforward – although the structure of the response functions becomes inherently more complex in this case (see [10]), the main features discussed here (i.e, diffusive spreading and narrowing of the cone) are still valid.

Finally, we have not been able to determine analytically the histogram for local stresses within the random BCC model. The major unsolved problem is the presence of negative forces, which induce a mechanical instability, and imposes that an extra rule should be added to the stochastic wave equation to determine how stress propagates. As emphasized above, we believe that this is a direct consequence of the tensorial nature of the problem and can be interpreted as a signature of “fragility” of the contact network, which is generically unstable to very small perturbations [3, 27].

ACKNOWLEDGEMENTS: We thank V. Bucholtz, E. Clément, J. Duran, C. Eloy and J. Rajchenbach for discussions.

References

- [1] R.L. Brown and J.C. Richard, 'Principles of Powder Mechanics' (Pergamon, New York, 1966).
- [2] L. Vanel, E. Clément, J. Lanuza and J. Duran, *Pressure screening and fluctuations in granular columns*, preprint.
- [3] P. Claudin and J.-P. Bouchaud, Phys. Rev. Lett. **78**, 231 (1997).
- [4] C.-h. Liu, S.R. Nagel, D.A. Scheeter, S.N. Coppersmith, S. Majumdar, O. Narayan and T.A. Witten, Science **269**, 513 (1995).
- [5] R. Brockbank, J.M. Huntley, and R.C. Ball, to be published in J. Phys. I (France).
- [6] D.M. Mueth, H.M. Jaeger and S.R. Nagel, *Force distribution in a granular medium* preprint
- [7] G.W. Baxter, in *Powder and Grains 97*, Behringer and Jenkins eds., Balkema, Rotterdam (1997).
- [8] see e.g. P. Dantu, Proc. of the fourth Int. Conf. On Soil Mech. and Found. Eng. (London 1957), **1** 144, Annales des Ponts et Chaussées, **IV**, 193 (1967), T. Travers et al., J. Phys. France, **49** 939 (1988).
- [9] S.N. Coppersmith, C.-h. Liu, S. Majumdar, O. Narayan and T.A. Witten, Phys. Rev. E **53**, 4673 (1996).
- [10] J.-P. Bouchaud, M.E. Cates and P. Claudin, J. Phys. I (France) **5**, 639 (1995).
- [11] J.P. Wittmer, M.E. Cates, P. Claudin and J.-P. Bouchaud, Nature (London) **382**, 336 (1996).
- [12] J.P. Wittmer, M.E. Cates and P. Claudin, J. Phys. I (France) **7**, 39 (1997).
- [13] H.A. Janssen, *Z. Vert. Dt. Ing.* **39**, 1045 (1895); see also R.M. Nedderman, *Statics and Kinematics of Granular Materials*, Cambridge University Press (1992).
- [14] F. Radjai, M. Jean, J.-J. Moreau and S. Roux, Phys. Rev. Lett. **77** 274 (1996); F. Radjai, D.E. Wolf, M. Jean and J.-J. Moreau, *Binomial character of stress transmission in granular packings*, preprint.
- [15] C. Eloy and E. Clément, to appear in J. Phys. I (France) (1997)
- [16] M. Nicodemi, *Force correlations and arches formation in granular assemblies*, preprint.
- [17] M. Chertkov, G. Falkovich and V. Lebedev, Phys. Rev. Lett. **76** 3707 (1996) and refs. therein.
- [18] M. Vergassola and A. Mazzino, *Structures and intermittency in a passive scalar model*, preprint.
- [19] L. Saul, M. Kardar and N. Read, Phys. Rev. **A** **45** 8859 (1992); D. Cule and Y. Shapir Phys. Rev. **B** **50** 5119 (1994).
- [20] S.F. Edwards and R.B. Oakeshott, Physica **D** **38**, 88-93 (1989); see also S.F. Edwards and C.C. Mounfield, Physica **A** **226**, 1,12,25 (1996).

- [21] J. Smid and J. Novosad, Proc. of 1981 Powtech Conference, Ind. Chem. Eng. Symp. **63**, D3V 1-12 (1981).
- [22] for a recent discussion on this approximation scheme and references, see, e.g. J.-P. Bouchaud, L. Cugliandolo, J. Kurchan and M. Mézard, Physica **A 226**, 243 (1996).
- [23] V. Bucholtz, J.-P. Wittmer and M.E. Cates, in preparation.
- [24] L. Landau and E. Lifschitz, 'Elasticity Theory', Pergamon Press.
- [25] O. Pouliquen, private communication.
- [26] P.-G. de Gennes, private communication.
- [27] In fact, fragility may arise even without disorder. The (noiseless) models of Refs. [10, 11, 12] predict that, in contrast to an elastic body, only certain combinations of boundary force can be supported by a given packing in static equilibrium; small deviations from these will cause rearrangement of the contact network. See, M.E. Cates, J.-P. Bouchaud, J.P. Wittmer and P. Claudin, in proceedings of Cargese School on Dry Granular Matter, H. Herrmann Ed., to be published.